NASA Technical Memorandum 104482

Particle Image Velocimetry for the Surface Tension Driven Convection Experiment Using a Particle Displacement Tracking Technique

Mark P. Wernet and Alexander D. Pline
Lewis Research Center
Cleveland, Ohio

Prepared for the
Fourth International Conference on Laser Anemometry
cosponsored by the American Society of Mechanical Engineers and the European Association for Laser Anemometry with organizational collaboration and sponsorship from Case Western Reserve University, Cleveland State University, NASA Lewis Research Center, and the Ohio Aerospace Institute
Cleveland, Ohio, August 5-9, 1991

NASA

Particle Image Velocimetry for the Surface Tension Driven Convection Experiment Using a Particle Displacement Tracking Technique

Mark P. Wernet and Alexander D. Pline

National Aeronautics and Space Administration
Lewis Research Center
Cleveland, Ohio

Abstract

The Surface Tension Driven Convection Experiment (STDCE) is a Space Transportation System flight experiment to study both transient and steady thermocapillary fluid flows aboard the USML–1 Spacelab mission planned for 1992. One of the components of data collected during the experiment is a video record of the flow field. This qualitative data is then quantified using an all electronic, two–dimensional Particle Image Velocimetry technique called Particle Displacement Tracking (PDT) which uses a simple space domain particle tracking algorithm. The PDT system is successful in producing velocity vector fields from raw video data. Application of the PDT technique to a sample data set yielded 1606 vectors in 30 seconds of processing time. A bottom viewing optical arrangement is used to image the illuminated plane, which causes keystone distortion in the final recorded image. A coordinate transformation was incorporated into the system software to correct for this viewing angle distortion. PDT processing produced 1.8% false identifications, due to random particle locations. A highly successful routine for removing the false identifications has also been incorporated reducing the number of false identifications to 0.2%.

Introduction

The Surface Tension Driven Convection Experiment (STDCE) is a fluid physics experiment to determine the nature and extent of transient and steady thermocapillary flows in the reduced gravity environment of low earth orbit aboard the Space Shuttle. The STDCE is manifested for flight on the United States Microgravity Laboratory–1 Space Shuttle mission, planned for 1992. Thermocapillary flow, or surface tension driven flow, is generated by a thermally induced surface tension variation along a liquid–gas interface. The surface tension gradient, established by non–uniform heating the free surface, is a surface tractive force, which creates a flow parallel to the liquid–gas interface from regions of low surface tension to high surface tension. Thermocapillary flows are important in technological applications where free surfaces are inherent and gravitational forces are small compared to capillary forces[1], such as containerless processing and crystal growth in low gravity, and terrestrial welding. Under certain circumstances periodic flow oscillations can occur[2-3] which are considered to be detrimental to the above processes.

The primary data returned from the STDCE are the surface temperature distributions and the qualitative velocity fields which are essential for determining the nature and extent of the thermocapillary flow. Therefore, it is imperative that the method of recording and analyzing the flow data be able to provide continuous qualitative and quantitative data. During the STDCE, the non–oscillatory flow field (studied predominantly in this flight) is 2–D, greatly simplifying the task of quantitative study. The Particle Image Velocimetry (PIV) technique of recording light scattered from small seed particles following the flow is well suited for this application. A variety of PIV schemes are available to both record and process the acquired data.[4-6] Many of these methods which utilize traditional photographic recording techniques and sophisticated processing hardware to produce quantitative data, add to the complexity of the experiment and are time consuming and expensive. Because of the additional complexity associated with designing and operating an experiment aboard the Shuttle, photographic plates or film are not practical in this environment. In addition, a standard RS–170 video system is part of the Shuttle complement of standard equipment, and is available for use during the STDCE. Also, near real time qualitative observation and quantitative analysis of the flow field by the ground crew are required. Therefore, standard video was chosen as the imaging and recording medium for the PIV images.

Qualitative video data obtained from the Charged Coupled Device (CCD) video camera in the STDCE will be processed via the Particle Displacement Tracking (PDT) technique.[7-10] The PDT technique is an all electronic technique which employs a single large memory buffer frame grabber board to digitize PIV images from an RS–170 video source. A time sequence of single exposure images are time coded into a single image using a simple
encoding scheme and then processed to track particle displacements and determine velocity vectors. All of the data acquisition reduction and analysis is performed on a 33MHz 80386 PC; no array processors or other processing hardware are required.

The data presented in this paper were produced using the STDCE flight hardware during the final testing of the flow visualization system. This data represents the culmination of an extensive testing program to determine a suitable camera/light source/particle size/particle concentration combination. The values of the above parameters were chosen based on optimum results obtained using the PDT system.

Particle Displacement Tracking Technique

The Particle Displacement Tracking (PDT) technique described here is applicable to low velocity ($\leq$ 20 cm/s), sparsely seeded PIV fluid flow systems, and is therefore ideally suited for the STDCE. In the PDT system, a cw laser source is used to generate a light sheet, and a video array camera/frame–grabber board records the particle image data. The frame–grabber board is used to acquire five video fields equally spaced in time from the RS–170 video source. The choice of five fields minimizes the error rate in subsequent processing.[7] The time interval, ΔT, between recorded fields is 1/60 second at the minimum, and essentially unlimited at the maximum time interval, which corresponds to the minimum velocities. The actual value of ΔT is selected according to the fluid velocities of interest. The particle seeding number density is selected so that the individual particles are clearly imaged.

The five video fields are then individually processed to determine the centroid location of each particle image on each

video field in the sequence. The particle centroid information is sufficient to determine the displacement of the particles between exposures. The particle image amplitude and shape information are used in estimating the centroids and subsequently discarded. The particle image centroids are estimated to within ± ½ pixel.[7] Although the particle positions are actually estimated to sub–pixel accuracy, at this point in the PDT development the need for high precision particle position estimates is not required. A simple boundary following algorithm is used to identify the individual particle images. Each particle image centroid is computed using the particle image light intensity distribution. The details of the centroid processing and estimation are discussed in Appendix I. The single pixel particle centroid estimates from all of the particle images recorded in the five field sequence are combined into a single 640×480×8 bit binary file. The time history of each particle image is encoded in the amplitude of the pixel marking the position of the particle centroid. The pixel amplitudes are coded according to the time order in the five field sequence. All of the particle centroids from video field #1 are encoded into the composite binary file as pixels with amplitudes 2^1. Similarly, particle centroids from video field #2 are encoded with amplitude 2^2, etc. By amplitude coding the pixel locations of the particle centroids, a single 2–D array is generated which contains the time history displacements of all the particles recorded in the five field sequence over a total time interval of $4\Delta T$. Amplitude coding unambiguously defines the particle's direction of travel. The amplitude coding also decreases the probability of mistakenly identifying a particle image from a different particle as being part of another particle displacement record. Another advantage of using single exposure particle image fields is the elimination of particle image overlap, which typically restricts the lower limit of velocities which can be measured. By individually processing the particle image fields, particle images with large diameters relative to their displacement between exposures are easily tolerated. The only constraint on the minimum velocity is that the particle must travel at least one pixel between exposures.

The amplitude coded time history file serves as the input to the PDT algorithm. The algorithm begins by scanning the time history file and storing the locations of all pixels with amplitude 2^1, which correspond to all particle positions at the initial field in the sequence, T=0 and serve as the starting point for the displacement tracking. By determining the displacement of the particle from its initial position, the velocity information of the flow is inferred.

For each initial particle position, a circular search region is defined around the 2^1 amplitude pixel. Inside the search region, the coordinates of all pixels with amplitudes equal to 2^2 are stored. The 2^2 amplitude coded pixels correspond to the particle positions at $T=1\Delta T$, or exposure #2. The detected 2^2 amplitude pixels within the search region are now each successively analyzed. The distance and angle between each 2^2 amplitude pixel and the search region center 2^1 amplitude pixel are computed and used to project where the 2^3, 2^4, and 2^5 amplitude pixels are located which correspond to the 2^1 and 2^2 amplitude pixel particles (Figure 1). If the projected pixel locations for the 3rd, 4th, and 5th particle images contain the corresponding amplitudes (2^3, 2^4, 2^5) then a complete particle displacement record has been detected. The velocity vector associated with this particle is computed from the distance between the initial and final particle locations (2^1 and 2^5 amplitude pixels) and the sum of the four inter–exposure intervals ($4\Delta T$). The detected particle pixel amplitudes are then set to zero. If the projected particle locations detect the incorrect pixel amplitude or zero amplitude, then the 2^2 amplitude pixel within the search region is not the actual second image of the 2^1 amplitude pixel at the center of the search region. Each 2^2 amplitude pixel within the search region is examined until a complete particle displacement pattern is detected or all of the 2^2 amplitude pixels are exhausted. If no match is found, the algorithm continues on to the next initial particle position 2^1 amplitude pixel. As a result of the search procedure no preknowledge about the flow system is required. The PDT system assumes that 2^2 amplitude pixels in the neighborhood of the initial 2^1 amplitude pixel are the most probable particle displacements between video fields #1 and #2 in the five field sequence. The maximum allowable particle displacement between exposures has previously been determined to be approximately 1.4" of flow angle change per pixel of displacement, or a maximum displacement of 10 pixels.[7] Ten pixel displacements between exposures minimizes the deviation of the particle path from a linear trajectory. Therefore, the search region size is defined to be a circle of radius 10 pixels (Figure 1).

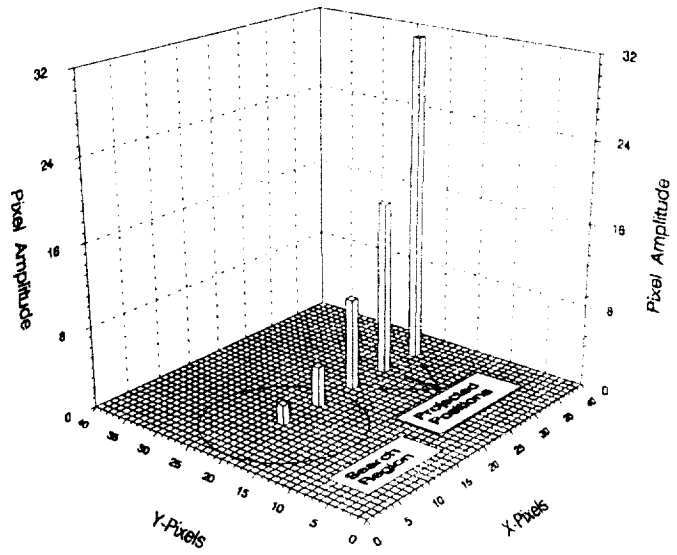

Figure 1 PDT time history coded pixel amplitudes and search region. Pixels with amplitude 2^2 within the circular search region are used to project where the 2^3, 2^4, and 2^5 particles are located. The projected particle positions must occur within the 3×3 search regions.

The positioning error on the discrete grid must be accommodated in the PDT processing. As previously mentioned, the boundary processing technique provides particle centroid estimates to within ± ½ pixel on the 640×480 pixel time history image. For each projected particle position (for exposures 3, 4, 5) a 3×3 pixel search region is defined. The 3×3 search regions are centered on the projected positions (Figure 1), allowing for the positioning error of ± ½ pixel. However, when a complete particle displacement pattern is detected, the exact location of the amplitude coded pixel within the 3×3 region is used to determine the velocity vector magnitude. The velocity vector angle is computed from the position of the 2^1 and 2^5 amplitude pixels.

The random locations of independent particle images on the time history image frame can be misconstrued as originating from a single particle, which results in a false velocity vector identification. The main factor affecting the number of false identifications is the particle number density in the fluid. The number of false identifications are greatly reduced by using the particle time history information. The particle arrival rate within the light sheet is governed by Poisson statistics. Assuming that the particle images are uniformly distributed across the recorded image, and that the particle number density

on each field in the five field sequence is roughly the same, then the number of particle images searched is:

$$N_1 = N\bar{\rho}\epsilon_p^2 \quad (1)$$

where: N Total number of pixels in recorded image
$\bar{\rho}$ Average particle number density in an exposure
ϵ_p^2 Pixel area

The user specifies the search region size corresponding to the maximum anticipated velocity to be measured. The search region is a circular area centered about the initial 2^1 amplitude pixel particles. Hence, for each 2^1 particle image searched, there are N_2 2^2 amplitude pixel particles in the circular search region which are scanned:

$$N_2 = \pi r^2 \bar{\rho}\epsilon_p^2 \quad (2)$$

where r is the radius of the circular search region. The probability of a particle being located within one of the projected 3×3 pixels search regions is given by:[7]

$$p = 1 - \epsilon^{-\bar{\rho}9\epsilon_p^2} \quad (3)$$

where $9e_p^2$ is the area of the 3×3 pixel projected search region. The total number of velocity vectors checked is the product of N_1 and N_2. The probability of detecting the correct amplitude pixels in each of the three projected search regions is given by equation 3. Hence, the total expected number of false identifications is given by:

$$\langle V_f \rangle = N\pi r^2 \bar{\rho}^2 \epsilon_p^4 \left[1 - e^{-\bar{\rho}9\epsilon_p^2}\right]^3 \quad (4)$$

For example, in a typical image field recorded from the experimental setup used in this work, the average number of particle images recorded was roughly 500particles/field. The imaged test cell covered 639×320pixels, which gives N=204480 and $\bar{\rho}$ = 500particles/204480pixel^2. The user specified search circular search region radius was 10pixels, and the pixel area equals unity. Using these values the expected number of false identifications is $\langle V_f \rangle$ = 0.004. In practice, typically 3–5% of the detected velocity vectors are false identifications for the flow field used in this study. The predicted error count is low due to the assumption of uniformly spaced particles, which does not strictly apply to the experimentally observed particle distribution. However, equation 4 provides the user with a gauge of the anticipated error rate as a function of the recorded particle number density, the user selected search region radius and the number of exposures used in the PDT processing algorithm.

There are two sources of error in the PDT estimated velocities: 1) the particle positioning error; and 2) the time interval error. The time interval error is minimal, since the frame–grabber board is genlocked to the RS–170 video signal from the video camera. The major source of error is from the particle centroid estimates. The total relative error in the measured velocity is given by:[7]

$$\frac{\sigma_U}{U} = \left[\left[\frac{\sigma_X}{X}\right]^2 + \left[\frac{\sigma_T}{T}\right]^2\right]^{\frac{1}{2}} \quad (5)$$

where U is the estimated mean velocity magnitude, X is the total particle displacement from the first to last exposures, T is the sum of the four time intervals $4\Delta T$, σ_X is the rms error in the total particle displacement, and σ_T is the timing error. For the ± ½ pixel positioning error, the rms error in the total displacement is simply $1/\sqrt{2}$ pixels. A nominal estimate for the time interval error is one video scan line per acquired field, or roughly 5×65μsec. Hence, for a 40 pixel total displacement and a minimum time interval of $\Delta T = 1/60$ sec, which corresponds to a total time interval from the first to last exposures of 1/15 sec, the relative error in the estimated velocity is:

$$\frac{\sigma_U}{U} = \left[\left[\frac{1/\sqrt{2}}{40}\right]^2 + \left[\frac{325E{-}6}{1/15}\right]^2\right]^{\frac{1}{2}} \quad (6)$$

or

$$\frac{\sigma_U}{U} = 1.8\%$$

which is dominated by the positioning error. For the worst case corresponding to only a 4 pixel total displacement, the relative error in the estimated velocity magnitude is a factor of 10 larger, or σ_U/U = 18%.

The error in the estimated velocity vector angle is similar to the magnitude error. The angular error is given by:[7]

$$\sigma_\theta = \text{ARCTAN}\left[\frac{\sigma_X}{X}\right] \quad (7)$$

where X and σ_X are the particle displacement and rms error in the particle displacement, respectively. Using the same displacement of 40 pixels, the angular error is:

$$\sigma_\theta = \text{ARCTAN}\left[\frac{1/\sqrt{2}}{40}\right] \quad (8)$$

$$\sigma_\theta = 1.0^\circ$$

The worst case for the angle estimates is for the smallest displacements. The minimum displacement of 4 pixels yields an error of $\sigma_\theta = 10.0^\circ$.

A unique feature of the PDT technique is afforded by the use of a large memory buffer frame–grabber board which can digitize individual fields at 1/60 second intervals and store 25 sequentially acquired video fields. The 25 fields are grouped in successive sets of 5 fields and processed by the PDT technique described above. The five groups of 5 successive fields produce five 2–D velocity vector maps. Particles are tracked across all five groups, for all 25 fields. Hence, the composite 2–D velocity vector map will track particles for all five groups of 5 frames. Particles tracked for all 25 fields will be represented by a string of velocity vectors oriented head to tail, which indicates the particle path over the total measurement time of $24\Delta T$. Alternatively, the five 2–D velocity vector data sets can be successively displayed at a user selected interval on a computer screen to elucidate the flowing fluid pattern.

Particle Displacement Tracking Software

The PDT data acquisition program is menu based, and offers the user several options for data acquisition. When acquiring an image sequence, the user is prompted for a file name root and the number of video fields to elapse between the acquired video fields. Both 5 and 25–field image sequences can be acquired with the inter–field acquisition time in multiples of 1/60 second. For low velocity flows many video fields are allowed to elapse between successively acquired images. For faster flows, adjacent fields can be acquired resulting in the minimum ΔT of 1/60 second. When acquiring adjacent fields, a gated camera may be required to obtain sharp particle images, otherwise particle streaks will be recorded instead. Two other operations available from the data acquisition program are used for determining the boundaries of the STDCE test cell in the recorded image, and for determining the requisite processing

threshold level.

The coordinates obtained from the reservoir boundary are used to delimit the region of the image to be processed to determine particle image centroids. Stray sources of light outside the reservoir are eliminated by defining the reservoir as a subregion of the recorded image. The background threshold level, determined via the data acquisition software, is used in the centroid processing program to eliminate background noise in the recorded image. The centroid processing algorithm requires that the particle images be distinctly defined, i.e. zero background level between particle images.

The recorded images from the STDCE are distorted due to the bottom viewing optical system. More detail concerning the origin of this distortion is presented in the Experimental Setup section. This distortion can be corrected numerically, after the recording stage in the centroid processing program. The particle centroid coordinates from the distorted image are transformed back to the rectangular object space. The coordinate transformation which accomplishes the correction is very simple and is described in more detail in Appendix II.

A plotting and data processing program, 'PDTGRAF', is used to analyze the PDT velocity vector data. The program lets the user analyze single, 5 and 25 field data sets or multiples of each. Data sets sampled with different inter–field times, ΔT, can be combined to produce graphs with high dynamic range.

The 'PDTGRAF' program offers an option to remove irregular, or falsely identified, velocity vectors from the data sets that have been selected for analysis. Not all data sets require the irregular velocity vector removal operation. If the original image quality was high, the particles uniformly distributed and not too dense, and a sufficiently high threshold level has been used, then very few incorrect identifications will be made. Typically, a few percent of the velocity vectors obtained will be falsely identified velocity vectors. The main premise used in the irregular vector removal algorithm is that there are a sufficient number of 'good' velocity vectors surrounding the 'bad' velocity vectors. The mean 'good' qualities are used to eliminate the falsely identified velocity vectors.

For each velocity vector in the selected data sets, the irregular vector removal operation determines the 10 nearest neighboring velocity vectors from the test vector coordinate. The mean u and v velocity components are computed from the 10 nearest neighbors and used to determine the validity of the velocity vector under test.

The 'PDTGRAF' program has two graph formats, a general format which displays the full 640×480 image acquired by the frame–grabber, and an STDCE specific format which displays only the pixels in the defined 2:1 aspect reservoir within the image. The reservoir is drawn with scaled dimension of 0 to 1 in the z/Z vertical axis, and 0 to 1 in the normalized r/R radial coordinate axis. Several lines of header information are drawn above the graph indicating the type of data processing selected, the number of raw velocity vectors read from the data files, and the pixel coordinates of the reservoir boundaries in the recorded image.

The 'PDTGRAF' program provides both on–screen graphics up to 1024×768 resolution and HP–Laserjet hard copy support at 300 dpi.[13] A few of the graphing options are only available on the graphics screen. The raw velocity vectors can be drawn in monochrome on the screen, or, if a 5–frame series has been read in, then the velocity vectors can be color coded to indicate in which frame in the series they belong. Another option available for the five frame series data is to rapidly display the time series of data vectors as successive 'movie' frames. By displaying each time ordered velocity vector data frame in succession, the fluid motion over the measurement period is observed.

Three data processing options are available in 'PDTGRAF': interpolation, velocity vector magnitude contouring, and stream line computation. The interpolation processing option sorts the velocity vector data to find the 20 nearest neighbors to the grid point being computed. A weighted 2–D linear least squares calculation is performed to estimate the velocity vector at each grid point using a weighting factor equal to the inverse square of the distance to the velocity vector. Grid sizes up to 64×64 can be accommodated. The interpolated vector field is used to calculate an iso–velocity magnitude contour map. The last data processing option is the stream function computation, which also starts with the interpolated vector field. The stream function is computed with the boundary condition $\Psi = 0$ at all boundaries, and the fluid surface velocity is restricted to the horizontal component, enforcing a non–deformable surface constraint. The stream lines are computed from the stream function and identified by labels normalized between −1 and 1. Positive streamlines indicate counter clockwise rotating flow, while negative streamlines represent clockwise rotating flow. Both the interpolated vector field and stream function data can be exported to data files to allow analysis by other means.

Equipment

An EPIX 4–MEG video frame–grabber board digitizes and stores the PIV images.[14] The frame–grabber board is equipped with a 12.5MHz A/D oscillator so that interlaced 640×480 square pixel frames are digitized. The frame–grabber board can be configured to digitize individual fields or frames. In field mode the minimum sampling time is 1/60 second. When acquiring video fields, 27 fields can be acquired and stored in the 4 Mbyte on–board memory buffer. However, by using just fields, the vertical resolution is halved, producing a 640 pixel × 240 line image. The 240 lines are the even or odd fields from the RS–170 interlaced video signal. The reduced vertical resolution decreases the accuracy of the particle centroid estimates in the vertical direction, compared to the horizontal direction. The reduced vertical sampling is not a significant effect if the particle images encompass several pixels across their diameters.

The data acquisition and PDT processing are all performed on a 33MHz 80386 computer with a Weitek 3167 coprocessor chip. All of the PDT processing routines are written in Fortran 77 and compiled with a 32 bit Weitek supported compiler. Video images are stored on the hard disk and later transferred to removable cartridge disks for archiving.

Experimental Setup

The PDT system has been used to evaluate various hardware configurations in order to optimize the quality of the PIV images produced by the STDCE. The extensive testing program, culminating with this data, has led to changes from the original design of the flight hardware.[11-12] The current hardware configuration is shown schematically in Figure 2. A variable focus beam produced by an RF–excited CO_2 laser, operating at 10.6 μm and absorbed within 0.2 mm of the free surface, was used to heat the fluid and generate the temperature gradient which drove the flow. The 3 W, 10 mm diameter beam was delivered at normal incidence to the free surface.

Because the STDCE flow field is (predominantly) 2–D, only a cross section of the test cell is illuminated with a sheet of light formed by passing the output of a 200 mW laser diode, operating at 800 nm, through a series of lenses and prisms. Two light sheets overlap to make a single light sheet which spans the

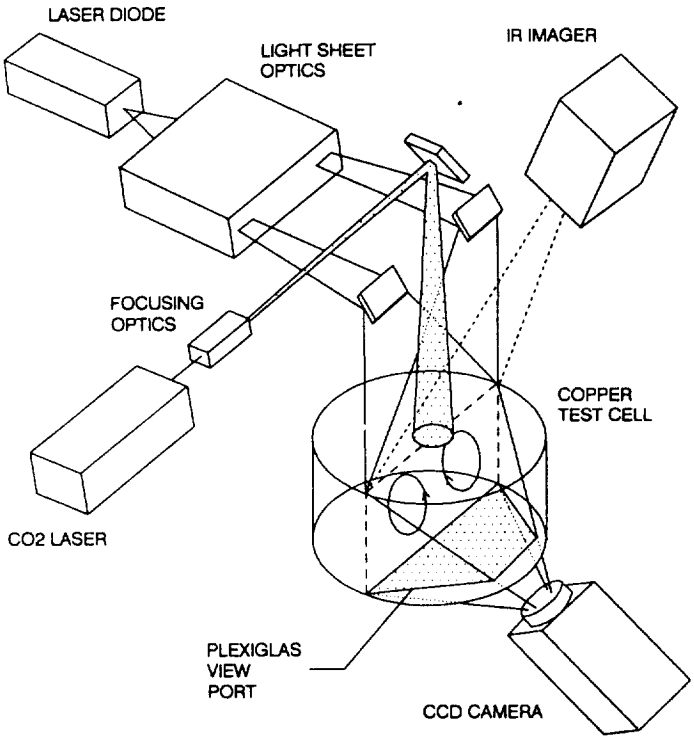

Figure 2 Schematic view of the Surface Tension Driven Convection Experiment.

entire test cell. This optical arrangement was necessitated because the heating beam must be in the same plane as the laser sheet.

A 10 cm diameter by 5 cm deep cylindrical copper test cell was chosen to contain the working fluid because the high thermal conductivity of copper is needed to maintain a constant side wall temperature, eliminating the possibility of optical access to the laser sheet at normal incidence. Therefore, a plexiglas bottom wall was designed with a precise shape to compensate for distortion caused by refraction of the light rays as they pass through the window into the camera. The only remaining distortion is caused by viewing the test cell cross section at an angle of 45°, referred to as keystone distortion, resulting in a non–linear, non–cartesian flow system, as imaged on the camera sensor (Appendix II).

The flow was seeded with 50–60 μm alumina (Al_2O_3) particles using an optimal concentration of 7.65×10^{-2} mg/ml. Because the size of these particles resulted in a high settling velocity ($\approx 10^{-1}$ mm/s) when used with the desired 10 centistoke silicone oil (for the flight experiment), a higher viscosity oil ($\approx$ 50 centistokes) was used only for these tests, to eliminate settling and verify the operation of the imaging system.

A 610 H by 488 V pixel array CCD camera fitted with a 6.5 mm diameter objective lens was placed at a 45° angle to the light sheet. The RS–170 video signal was recorded on a 3/4" tape Video Cassette Recorder (VCR).

Before the data acquisition, 30 ml of a solution containing 1 mg/ml of tracer particles suspended in the working fluid was added to the 392 cc of clean oil in the test chamber. The mixture was stirred until the particles were uniformly distributed. After the flow became quiescent the CO_2 laser beam was unblocked starting the flow. Data was acquired for approximately one minute thereafter.

Results and Discussion

Because the STDCE flow field has a very high dynamic velocity range, six 25 field data sets were digitized from the same section of videotape. Each set of 25 fields was used to generate time evolved velocity vectors. The data sets consisted of inter–field times (IFT), the time between successively acquired fields, of 10, 20, 30, 40, 60, and 80 fields, yielding a

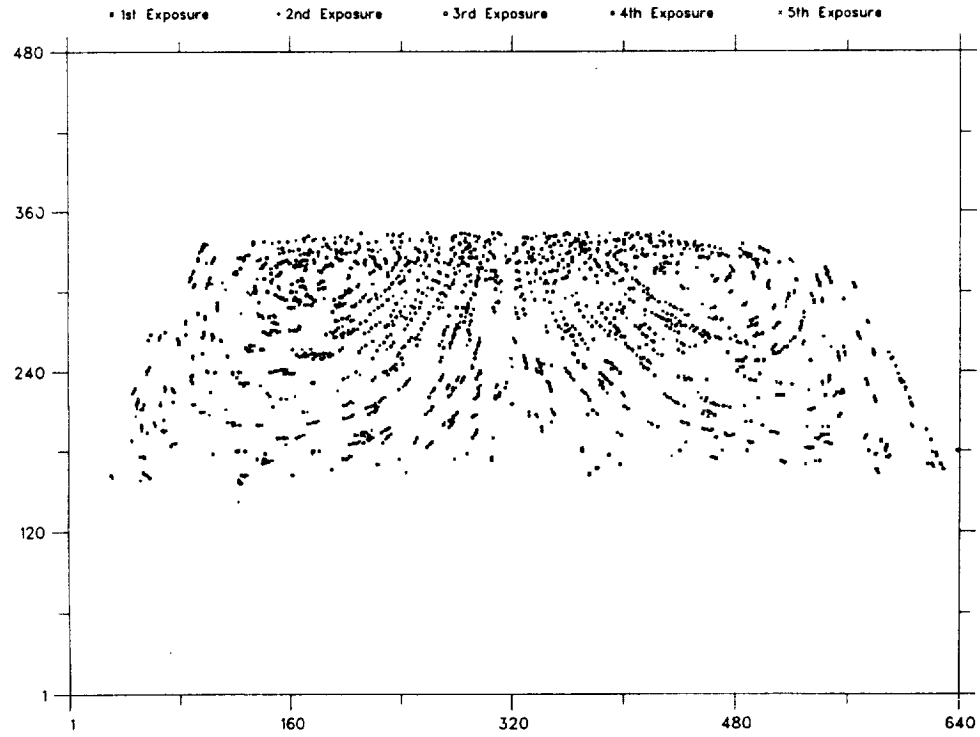

Figure 3 Time history coded particle image centroids plotted in pixel coordinates: keystone distorted coordinate system. The key at the top of the graph defines the symbol coding.

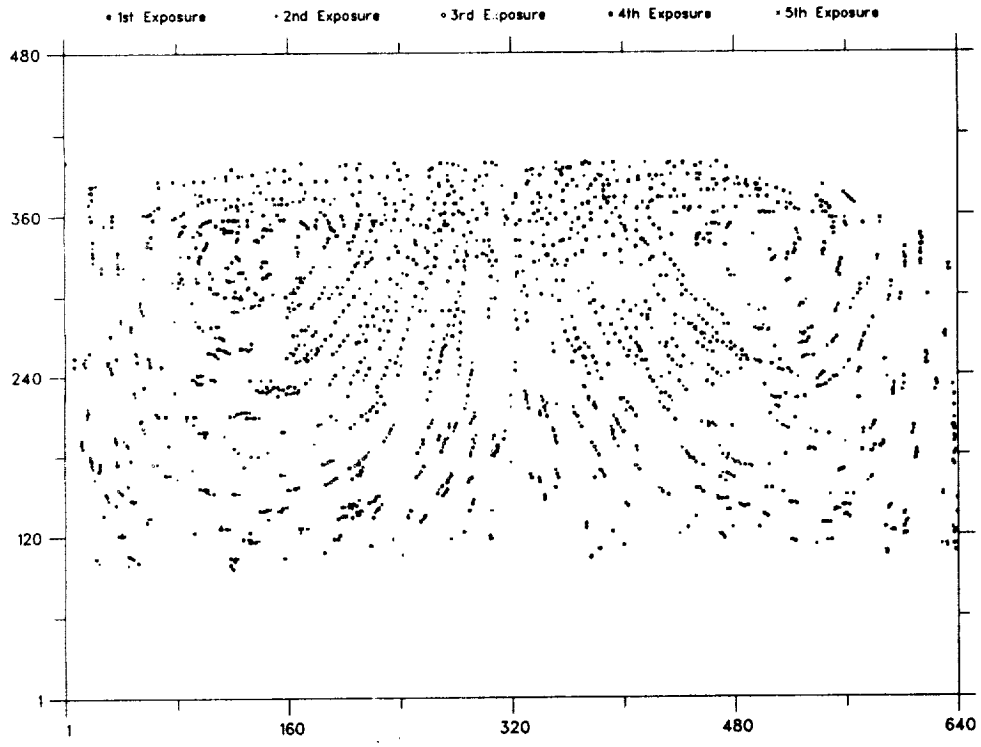

Figure 4 Time history coded particle image centroids plotted in pixel coordinates: cartesian coordinate system.

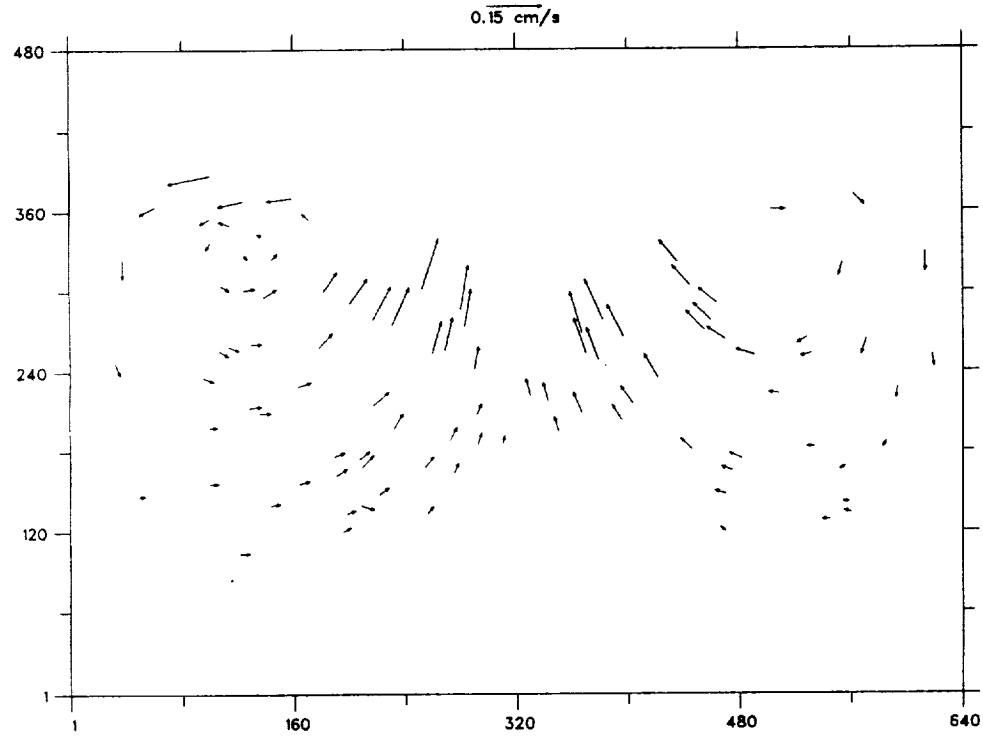

Figure 5 Raw velocity vectors from the 60 IFT data set corresponding to the particle image centroids shown in Figure 4, plotted in pixel coordinates.

dynamic range of 80:1.[10] The STDCE flow structure dictates the need for this high dynamic range. The total acquisition time for the 80 IFT data set was 32 seconds, with the higher velocity data sets taking proportionately less time. Since the flow structure does not change appreciably during this time, the resulting vector plot of the combined data sets can be assumed to be from the same instant in time.

The data sets were boundary processed to determine the particle image centroids using a threshold of 50 grey levels to remove background noise from the digitized images, detecting approximately 400 particles per field. During this step the particle image centroids are transformed from the keystone distorted coordinate system to a cartesian system. Figures 3 and 4 illustrate the particle image centroids in both the keystoned and cartesian coordinate systems from the first group of 5 digitized images in the 60 IFT data set. The centroids are plotted in pixel coordinates from the frame–grabber board (640 h × 480 v), where 1 cm equals 64 pixels (156 μm/pixel). Note the five exposure sequences (□ + ○ • ×) in the cartesian system are much more spread out, and therefore less likely to produce falsely identified vectors due to random centroid locations.

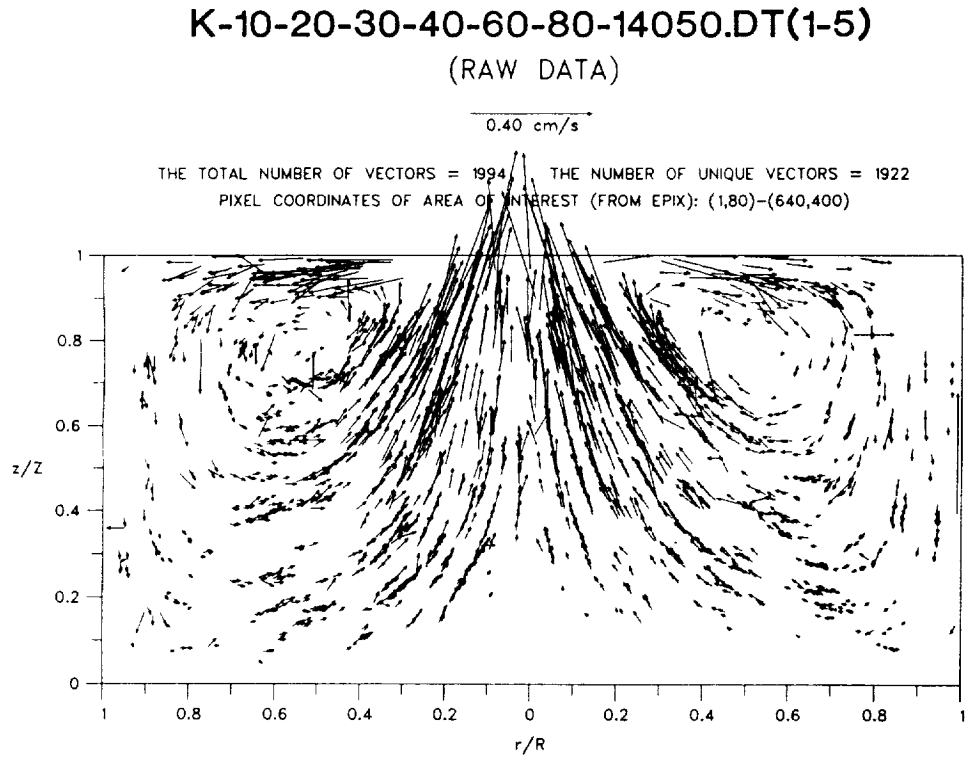

Figure 6 Raw velocity vector plot consisting of 6 combined data sets plotted in non–dimensional coordinates corresponding to the STDCE cell geometry.

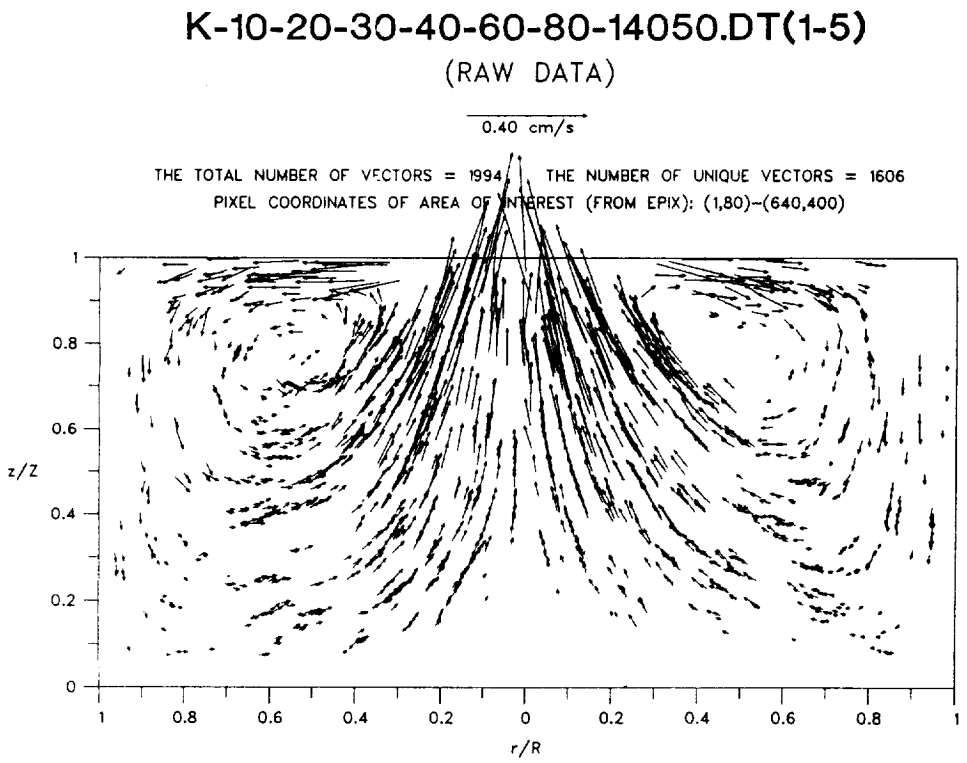

Figure 7 Velocity vector plot consisting of 6 combined data sets with false identifications removed plotted in non–dimensional coordinates.

Next the PDT processing was performed on the particle centroid locations from all six data sets in a serial batch mode without intervention, freeing the operator for other tasks. Figure 5 shows the 97 resulting velocity vectors from the particle centroids shown in Figure 4. The combination of the 6 data sets yielded 1994 vectors. The CPU time required for the PDT processing for all six data sets was 30 seconds. The total time required for boundary and PDT processing for all six data sets was approximately 3.5 minutes, of which 60% is disk file access time.

The 'PDTGRAF' data analysis program was then used to refine, plot and analyze the raw velocity vector information. Routines for removing duplicate vectors, false identifications, plotting in non–dimensional coordinates, interpolating velocity vectors, calculation of iso–velocity contours and the stream function are included in 'PDTGRAF'.

When adding multiple data sets, velocity vectors could have been recorded at the same spatial location. Accordingly, duplicate vectors, vectors having the same x,y coordinate, are

averaged together, yielding 1922 velocity vectors. This raw data is shown in Figure 6, plotted in non–dimensional coordinates described in a previous section. The title 'K–10–20–30–40–60–80–14050.DT(1–5)' represents all the salient information from the 6 data sets, where K is the particular hardware configuration, '10–20–30–40–60–80' are the IFT's, '14' is the data run #, '050' is the threshold value used for processing, the file extension '.DT' indicates that the keystone correction has been implemented and '(1–5)' illustrates that 25 field data sets (5 groups of 5) have been used. The maximum velocity found in the data sets was 0.40 cm/sec indicated by the scale under the title. The vortical flow structure is clearly depicted in this plot. The choice of the selected IFT's captures both the faster moving return flow in the center of the cell and the slower flow down the side wall. Of the 1922 vectors in Figure 6, 1.8% are false identifications. The application of the irregular vector removal routine on the raw velocity vector data yielded 1606 vectors, of which only 0.2% are false identifications, an 90% reduction in false identifications. It is clear from a comparison of Figures 6 and 7 that even though some 'good' vectors are removed, the resulting refined plot is an excellent representation of the physical flow field.

Analysis of the randomly sampled experimental data is facilitated by interpolation and plotting on a user defined N×N regular grid. Figure 8 shows the result of applying the interpolation routine, using a 32×32 grid, to the refined velocity vector information shown in Figure 7. From the interpolated data the velocity profiles at various locations are readily evident and can be exported for easy comparison with flow calculations of the STDCE.

The 32×32 interpolated grid of velocity vectors is then used to calculate and plot iso–velocity contours and the stream function, shown in Figures 9 and 10. Note that, by definition, the velocity vector field should be, and is tangent to the stream function. The experimentally determined stream function is another result which can readily be compared with a computed flow to determine the similarity of the overall flow patterns.

Conclusions

The PDT technique is an all electronic, relatively simple method for determining low speed flow velocities, which circumvents the deficiencies associated with other PIV methods, such as chemical processing of photographic plates, specialized array processors and long turn around times. The PDT system produced 1222 independent velocity vectors from a section of raw video images acquired using a large memory frame–grabber board in 30 seconds on a 33MHz 80386 PC. The data were refined by removing falsely identified velocity vectors and interpolating onto a regular grid where associated iso–velocity and stream function plots were produced, the entire process requiring only minutes from start to finish. After careful comparison of this data with the original video data the results from the PDT system are an excellent representation of the physical flow, both qualitatively and quantitatively.

Acknowledgements

The authors would like to thank Don Buchele, David Van Zandt, Nora Bozzolo and Mike Lewis of the STDCE optical design team for their efforts in developing the flow visualization system.

References

1. S. Ostrach, "Convection Due to Surface Tension Gradients", *COSPAR Space Research*, Vol. 19, Pergamon, Oxford, England, 563–570, (1979).

2. Ch. H. Chun and W. Wuest, "Experiments on the transition from the steady to the oscillatory Marangoni–convection of a floating zone under reduced gravity effect", *Acta Astronautica*, 6, 1073, (1979).

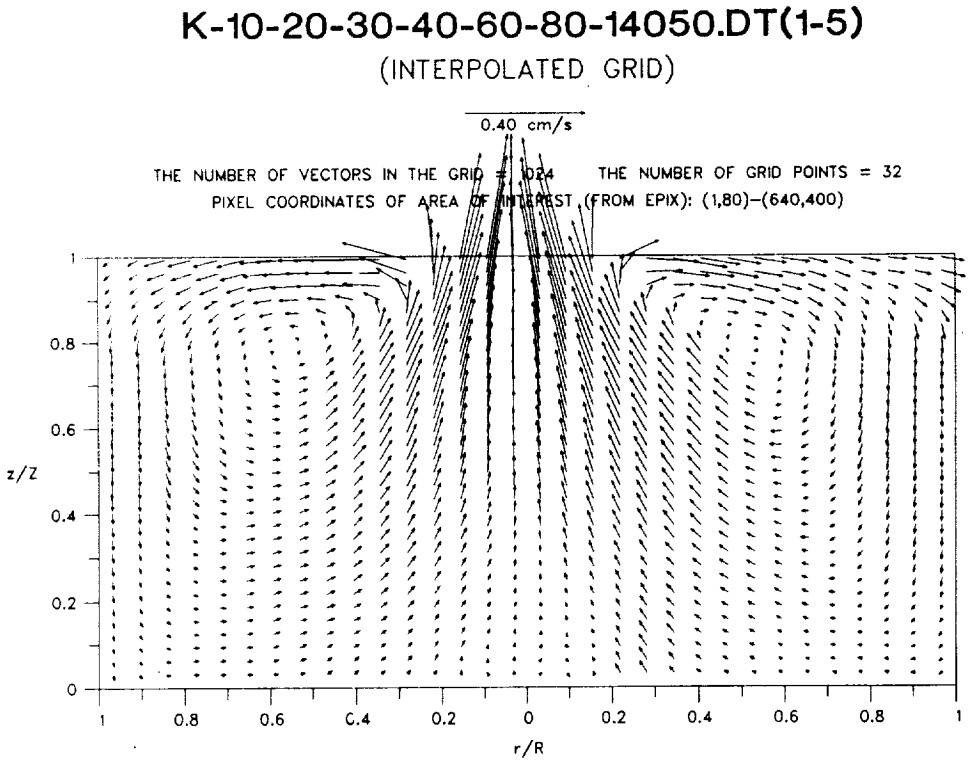

Figure 8 Interpolated 2–D velocity vector map plotted in non–dimensional coordinates. The 6 data sets have been interpolated over a 32×32 grid.

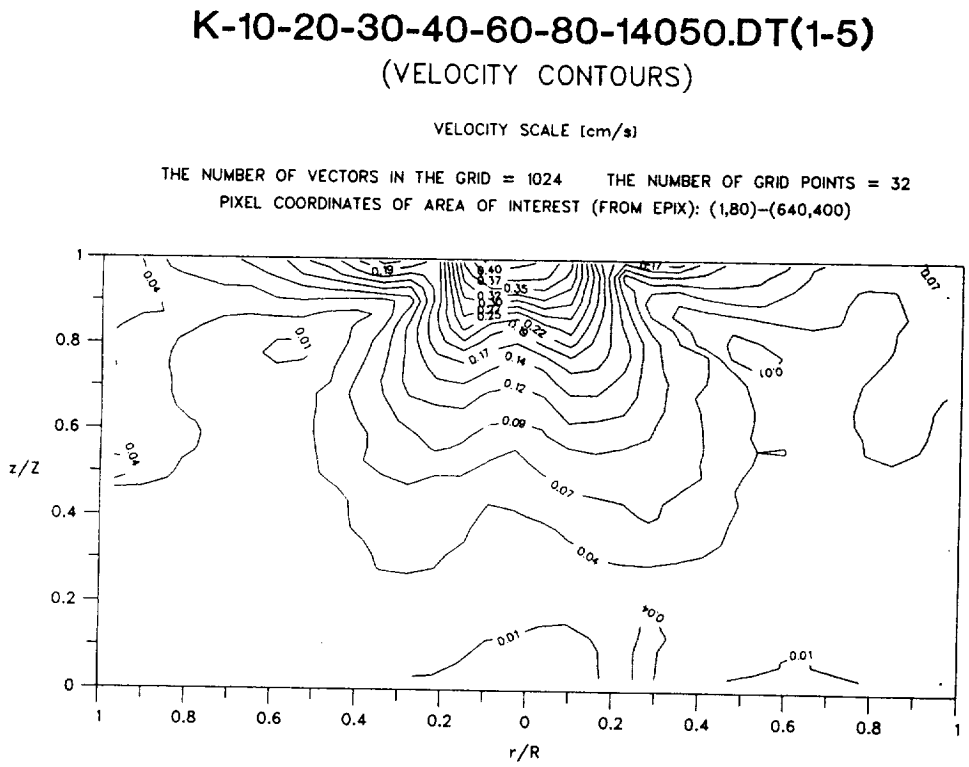

Figure 9 Iso–velocity contours plotted in non–dimensional coordinates. The 6 data sets have been interpolated over a 32×32 grid.

7. M. P. Wernet, " A new Data Reduction Technique for Pulsed Laser Velocimetry", Ph.D. Thesis, Case Western Reserve University, May, (1989).

8. M. P. Wernet and R. V. Edwards, "A Vector Scanning Processing Technique for Pulsed Laser Velocimetry", *19th International Congress on Instrumentation in Aerospace Simulation Facilities (ICIASF)*, Göttingen, West Germany, September 18–21, (1989) (Also NASA TM–102048).

9. M. P. Wernet and R. V. Edwards, "A New Space Domain Processing Technique for Pulsed Laser Velocimetry", *Applied Optics*, 29, 3399–3417, (1990).

10. M. P. Wernet, "Particle Displacement Tracking for PIV", *Applied Optics*, 30, (1990), (Also NASA TM–102388).

determine the minimum x and y extents, and the maximum x and y extents of the particle image. These limits are used to define a rectangular area which is integrated along the x and then y axes to determine the x and y–projections of the particle image. The particle image's intensity weighted mean x and y coordinates are computed from the respective projections. The particle image centroid coordinates, along with the current field number being processed are stored. The pixel amplitudes in the rectangular area delimiting the particle image are then set to zero amplitude. Setting the pixel amplitudes to zero avoids redetecting the particle image on a subsequent pass. The program then resumes searching in a left to right direction for the next non–zero pixel value. The entire bounded region of the image file is searched for particle image centroids.

The particle centroid data is then written to a time history file. The size of the time history file is 640×480 pixels, by 8 bits. The particle images are effectively 1 pixel in

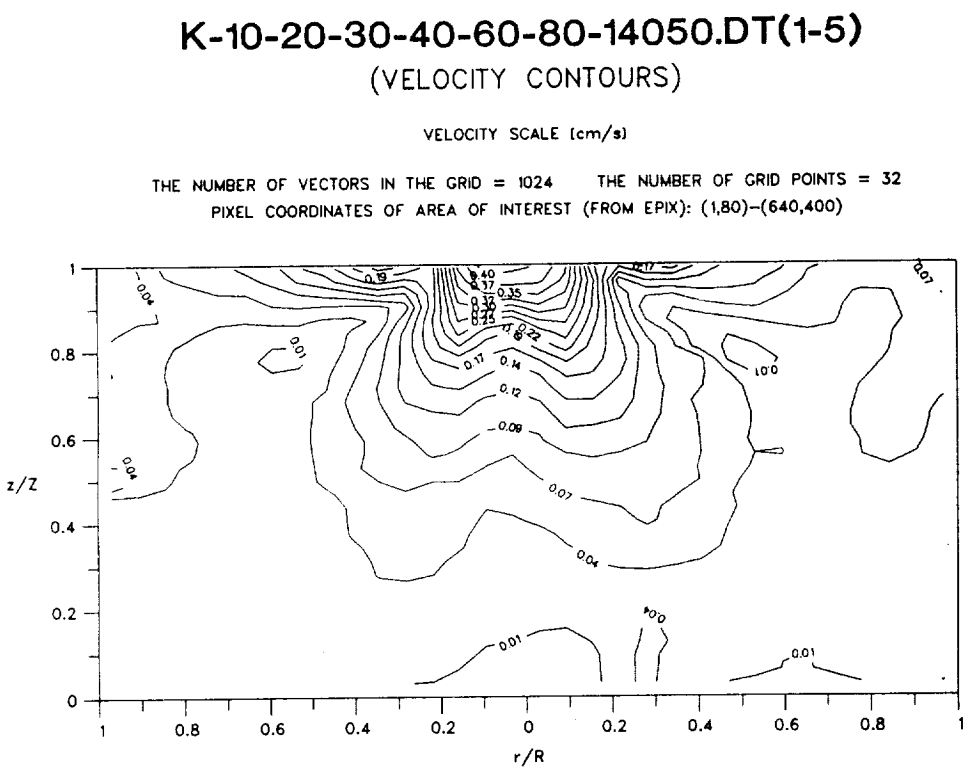

Figure 9 Iso–velocity contours plotted in non–dimensional coordinates. The 6 data sets have been interpolated over a 32×32 grid.

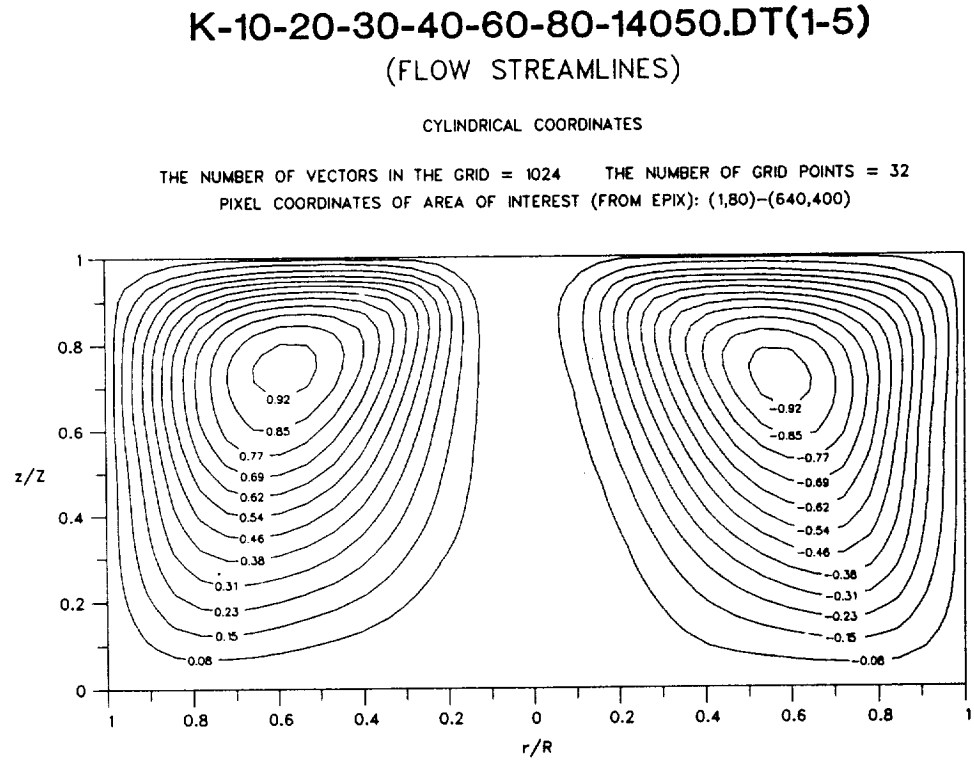

Figure 10 The stream function plotted in non–dimensional coordinates. The 6 data sets have been interpolated over a 32×32 grid with the contour labels normalized to ±1.

3. Y. Kamotani and K. J. Lee, "Oscillatory Thermocapillary Flow in a Liquid Column Heated by a Ring Heater", *PCH Journal*, 11, No. 5/6, 729–736, (1989).

4. R. J. Adrian, "Multipoint Optical Measurements of Simultaneous Vectors in Unsteady Flow– A Review", *International Journal of Heat and Fluid Flow*, 7, 127–145, (1986).

5. L. Lourenco and A. Krothapalli, "Particle Image Displacement Velocimetry Measurements of a Three Dimensional Jet", *Physics of Fluids*, 31, 1835–1837, (1988).

6. R. Höcker and J. Kompenhans, "Application of Particle Image Velocimetry to Transonic Flows", 5th *International Symposium on Applications of Laser Anemometry to Fluid Mechanics*", Lisbon, Portugal, Paper #15.1, (1990).

7. M. P. Wernet, " A new Data Reduction Technique for Pulsed Laser Velocimetry", Ph.D. Thesis, Case Western Reserve University, May, (1989).

8. M. P. Wernet and R. V. Edwards, "A Vector Scanning Processing Technique for Pulsed Laser Velocimetry", *19th International Congress on Instrumentation in Aerospace Simulation Facilities (ICIASF)*, Göttingen, West Germany, September 18–21, (1989) (Also NASA TM–102048).

9. M. P. Wernet and R. V. Edwards, "A New Space Domain Processing Technique for Pulsed Laser Velocimetry", *Applied Optics*, **29**, 3399–3417, (1990).

10. M. P. Wernet, "Particle Displacement Tracking for PIV", *Applied Optics*, **30**, (1990), (Also NASA TM–103288).

11. S. Ostrach and Y. Kamotani, "Design of a Thermocapillary Flow Space Experiment", *Journal of Thermophysics and Heat Transfer*, 1, No. 1, 83–89, (1987).

12. A. D. Pline, T. P. Jacobson, J. S. Wanhainen and D. A. Petrarca, "Hardware Development for the Surface Tension Driven Convection Experiment", *Journal of Spacecraft and Rockets*, **27**, No. 3, 312–317, (1990).

13. Halo Professional Programmer's Guide, Media Cybernetics, (1990).

14. EPIX 4–MEG Video Board Operator's Manual, EPIX Inc, (1990).

15. D. Buchele,"Analytical Correction of Keystone Distortion", ADF Memorandum, Task Order 45–21, NASA Contract NAS3–25767, (1990).

APPENDIX I

Particle Image Boundary Processing Algorithm

The boundary processing routine sequentially processes all 5 fields in the acquired sequence. The images to be processed are compared to the user supplied threshold level as they are read into the computer memory. The threshold level is set just high enough to remove the background noise from the CCD camera. The boundary search is initiated in the upper left corner of the image, searching from left to right for non–zero pixel amplitudes. When a non–zero amplitude pixel is detected, the program searches the particle image boundary in a clockwise manner. Starting at the initially detected non–zero amplitude pixel, the program looks at the pixel on the right, and then looks at the pixel below. If a non–zero amplitude pixel is found to the right, the program moves there. If a non–zero amplitude pixel is found below the current pixel, the program moves there. This search procedure (right–down) is repeated, and the coordinates of the upper right corner of the particle are recorded until the test fails. The program then switches to a look down, look left mode. This search precedence defines the lower right portion of the particle image perimeter, until a null case is found. The lower left corner of the particle image is found by a look left, look up precedence. When this search procedure obtains a null condition, the final search mode begins. The final search mode is a look up, look right, which defines the upper right corner of the particle. The search terminates when the initial search position is encountered. All of the detected non–zero particle image perimeter coordinates are stored.

Next, the program scans the perimeter coordinates to determine the minimum x and y extents, and the maximum x and y extents of the particle image. These limits are used to define a rectangular area which is integrated along the x and then y axes to determine the x and y–projections of the particle image. The particle image's intensity weighted mean x and y coordinates are computed from the respective projections. The particle image centroid coordinates, along with the current field number being processed are stored. The pixel amplitudes in the rectangular area delimiting the particle image are then set to zero amplitude. Setting the pixel amplitudes to zero avoids redetecting the particle image on a subsequent pass. The program then resumes searching in a left to right direction for the next non–zero pixel value. The entire bounded region of the image file is searched for particle image centroids.

The particle centroid data is then written to a time history file. The size of the time history file is 640×480 pixels, by 8 bits. The particle images are effectively 1 pixel in diameter, and the amplitude of the pixel indicates on which field in the 5–field sequence the particle was recorded.

The accuracy of the estimated particle image centroids depends upon the size and shape of the particle image. The particle image intensity distributions are assumed to be approximately Gaussian. The accuracy of the estimate is proportional to the width of the particle image in pixels. A Maximum Likelihood Estimation analysis has been performed for Gaussian shaped particle images and the results are reported in reference 7. In reference 7, a graphical representation of the variance in the particle image centroid estimate as a function of the ratio of the particle image standard deviation to pixel width is presented. The total energy content of the particle image is defined as α_1 and the particle image centroid location is defined as α_2. For a Gaussian distributed light intensity particle image, the e^{-2} diameter ($d_{e^{-2}}$) of the particle is defined as 4σ, where σ is the standard deviation of the Gaussian light intensity distribution. The pixel width is ϵ_p. Hence, α_3 can be defined as $\sigma/\epsilon_p = d_{e^{-2}}/4\epsilon_p$. For a typical particle image, which is nominally 5 pixels across ($\alpha_3 = 5/4 \cdot 1 = 1.25$), the estimated variance is $0.2 = \mathrm{Log}_{10}\{\alpha_1 Var(\alpha_2)\}$. Hence, $\sigma_{\alpha 2} = \pm 2.8/\alpha_1$, which means that the error in the estimated centroid decreases inversely with the recorded particle image intensity. A conservative estimate for the error in particle image centroid estimate is $\sigma_{\alpha 2} = \pm \frac{1}{2}$ pixels, which corresponds to a small image brightness. This value for the error estimate is used in all subsequent analysis of the estimates of the error in the measured velocity vectors. For more discussion of the errors in the measured velocity vectors see references 7 and 9.

The conservative estimate for the error in the centroid estimate above is used because, as mentioned previously in the discussion of the boundary processing routines, image fields are acquired by the data acquisition software. The image fields contain only 240 lines, thus each line of video is doubled as the image field files are read into the computer. Doubling the number of rows in the image has a minimal effect on the particle centroid estimates, down to 3 pixel wide particles. For particle images smaller than 3 pixels, the vertical estimate of the particle image centroid may be off by as much as ±1 pixel.

APPENDIX II

Keystone Correction

The bottom viewing restriction in the STDCE setup causes keystone distortion in the recorded image of the illuminated cross section of the fluid. The tilted object plane is imaged onto the CCD array via a camera lens. The camera lens is aligned with the optical axis of the object and image planes. The CCD array camera is slightly tilted relative to the lens. All

points in the object plane are in focus in the tilted image plane. The keystone effect arises because all points on the object are not the same distance from the lens, thus, the magnification of the object varies in the tilted plane of the image. The effective magnification, m, of an imaging system is given by the ratio $m = s_i/s_o$, where s_i is the image distance from the lens, and s_o is the object distance from the lens. The variation in the magnification is nonlinear due to the changing ratio of object to image distance. The plane normal to the tilted plane has constant magnification which is a function of the longitudinal magnification. The keystone distortion could be corrected optically before recording, but would require more space than is available for the imaging optics. Hence, the correction was chosen to be performed numerically after the image recording stage.[15]

In the STDCE setup, the 100mm wide by 50mm high illuminated cross section of the reservoir is imaged onto a CCD array. The base of the reservoir, which is closest to the lens, is imaged to the full width of the CCD imaging area. However, the top of the illuminated area is further away from the lens, and is therefore imaged with a smaller effective magnification (longer object distance, shorter image distance). The resulting keystone image of the rectangular illuminated cross section is an isosceles trapezoid.

The keystone correction for the rectangular object is very easily implemented. Three constants are used in the keystone correction transformation. The constants are computed using the coordinates of three corners of the recorded keystone image. No information about the optical system is required. Figure A1 shows the corners of the keystone image used to compute the constants. Primed quantities refer to coordinates on the keystone distorted image plane, while unprimed quantities refer to the object plane. The first constant sets the origin of the keystone image:

$$y_1' = x_1' \left[\frac{y_2'-y_1'}{x_2'-x_1'}\right] \qquad (A1)$$

The other two constants which relate the image to object are:

$$A = \frac{y_2 - y_1}{\left[\frac{1}{y_2'} - \frac{1}{y_1'}\right]} \qquad (A2)$$

$$B = \frac{x_1'}{x_1 \cdot y_1'} \qquad (A3)$$

The only unknown is y_2-y_1, which is not available in the keystone distorted image. Since the reservoir geometry is fixed at 2:1 (w:h), the width of the base of the isosceles trapezoid can be used to fix the height, y_2-y_1, of the corrected image. The constants need only be computed once. Then for any point x', $y'-y_1'$ in the keystone distorted image has coordinates in the object plane given by:

$$y-y_1 = A\left[\frac{1}{y'} - \frac{1}{y_1'}\right] \qquad (A4)$$

$$x = \frac{x'}{B \cdot y'} \qquad (A5)$$

The resulting image is corrected to the original rectangular 2:1 aspect ratio of the object.

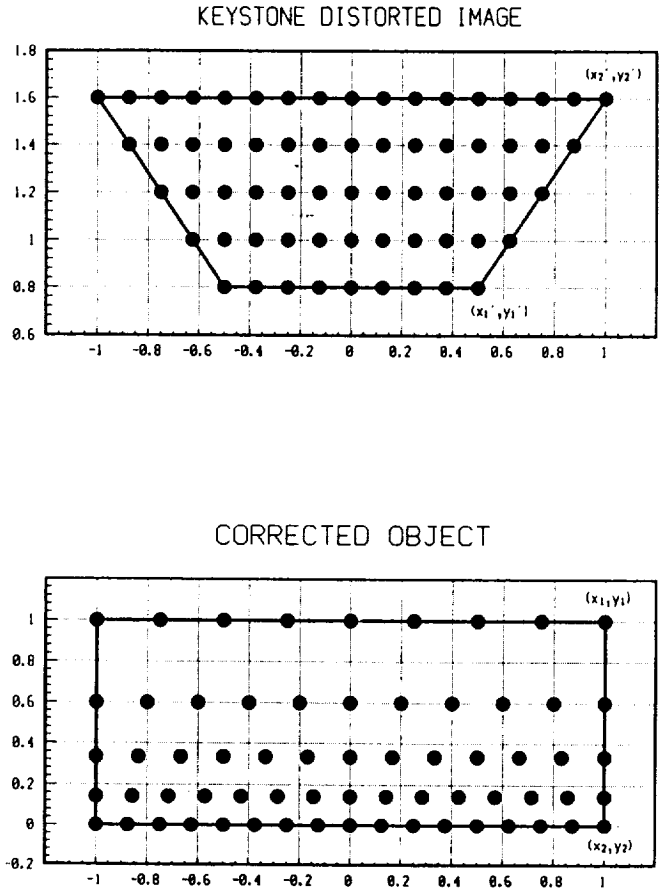

Figure A1 The top portion of the graph shows a representative keystone distorted image with uniformly spaced samples. The bottom graph shows the sampled image transformed to cartesian coordinates. Note the non–uniform spacing between points in the transformed image.

NASA
National Aeronautics and Space Administration

Report Documentation Page

1. Report No.	2. Government Accession No.	3. Recipient's Catalog No.
NASA TM-104482		

4. Title and Subtitle
Particle Image Velocimetry for the Surface Tension Driven Convection Experiment Using a Particle Displacement Tracking Technique

5. Report Date

6. Performing Organization Code

7. Author(s)
Mark P. Wernet and Alexander D. Pline

8. Performing Organization Report No.
E-6327

10. Work Unit No.
505-62-50

9. Performing Organization Name and Address
National Aeronautics and Space Administration
Lewis Research Center
Cleveland, Ohio 44135-3191

11. Contract or Grant No.

13. Type of Report and Period Covered
Technical Memorandum

12. Sponsoring Agency Name and Address
National Aeronautics and Space Administration
Washington, D.C. 20546-0001

14. Sponsoring Agency Code

15. Supplementary Notes
Prepared for the Fourth International Conference on Laser Anemometry cosponsored by the American Society of Mechanical Engineers and the European Association for Laser Anemometry with organizational collaboration and sponsorship From Case Western Reserve University, Cleveland State University, NASA Lewis Research Center, and the Ohio Aerospace Institute, Cleveland, Ohio, August 5-9, 1991. Responsible person, Mark P. Wernet, (216) 433-3752.

16. Abstract

The Surface Tension Driven Convection Experiment (STDCE) is a Space Transportation System flight experiment to study both transient and steady thermocapillary fluid flows aboard the USML-1 Spacelab mission planned for 1992. One of the components of data collected during the experiment is a video record of the flow field. This qualitative data is then quantified using an all electronic, two-dimensional Particle Image Velocimetry technique called Particle Displacement Tracking (PDT) which uses a simple space domain particle tracking algorithm. The PDT system is successful in producing velocity vector fields from the raw video data. Application of the PDT technique to a sample data set yielded 1606 vectors in 30 seconds of processing time. A bottom viewing optical arrangement is used to image the illuminated plane, which causes keystone distortion in the final recorded image. A coordinate transformation was incorporated into the system software to correct for this viewing angle distortion. PDT processing produced 1.8% false identifications, due to random particle locations. A highly successful routine for removing the false identifications has also been incorporated reducing the number of false identifications to 0.2%.

17. Key Words (Suggested by Author(s))	18. Distribution Statement
Particle trajectories Velocity measurement	Unclassified - Unlimited Subject Category 35

19. Security Classif. (of the report)	20. Security Classif. (of this page)	21. No. of pages	22. Price*
Unclassified	Unclassified	12	A03

NASA FORM 1626 OCT 86

*For sale by the National Technical Information Service, Springfield, Virginia 22161